Articles

Reaction of Phosphines and Pyridine with a Heterometal Metallaborane. Ligand Substitution on Boron vs Metal Sites, Borane Displacement, and Orthometalation of a Boron-Coordinated Pyridine

Xinjian Lei, Maoyu Shang, and Thomas P. Fehlner*

Department of Chemistry and Biochemistry, University of Notre Dame, Notre Dame, Indiana 46556-5670

Received August 2, 2000

The reactions of the mixed-metal metallaborane $\{Cp^*Ru\}\{Cp^*Ru(CO)\}\{Co(CO)_2\}(\mu\text{-}CO)\text{-}B_3H_6$, **1**, $Cp^* = \eta^5\text{-}C_5Me_5$, with PPh_3 and PMe_2Ph as representative phosphine bases and pyridine as a representative nitrogen base have been studied. Phosphines lead to substitution of CO on Co and the formation of $\{Cp^*Ru\}_2\{Co(CO)L\}(\mu\text{-}CO)_2B_3H_4$, $L = PPh_3$ (**2**) and PMe_2Ph (**3**). The latter has been structurally characterized in the solid state and exhibits the fac isomeric form of an octahedral M_3B_3 cluster. NMR data demonstrate that **3** is fluxional in solution and exists in two isomeric forms: in the major one the phosphine is adjacent to the B_3 face, and in the minor one it is adjacent to the M_3 face. Reaction with pyridine leads to three products, two of which have been characterized by X-ray structure determinations. Formation of $\{(Cp^*Ru(CO)\}\{Co(CO)_2\}(\mu\text{-}CO)\{Cp^*\overline{Ru\}B_2H_2(NC_4H_4C)}$, **4**, demonstrates borane fragment displacement plus pyridine addition and subsequent orthometalation. Formation of $\{Cp^*Ru\}_2\{Co(CO)_2\}(\mu\text{-}CO)_2B_2H_2B(NC_5H_5)$, **5**, establishes a parallel pathway involving H substitution on boron accompanied by hydrogen elimination.

Introduction

The reactions of polyhedral boranes with Lewis bases constitute a substantial fraction of their chemistry.[1,2] Cage opening,[3] borane displacement,[4] and deprotonation[5] are three well-documented reactions. Likewise, transition metal clusters undergo a similar rich chemistry with Lewis bases,[6] cluster opening,[7] metal fragment displacement,[8] and deprotonation[9] parallel to those of borane cages. In addition, when metal clusters possess monodentate ancillary ligands, ligand substitution is a prominent reaction pathway.[10]

Metallaboranes[11−14] offer similar possibilities but with the added feature of competition between metal and boron sites for the base, i.e., borane displacement vs metal fragment displacement, ligand substitution at boron vs metal sites, removal of M−H−M vs M−H−B vs B−H−B protons, etc. In addition, for bases incorporating aromatic rings, orthometalation to adjacent metals,[15] as well as adjacent boron atoms,[16] can play a role in determining the final product. Some systematic studies of these aspects of metallaborane chemistry have appeared;[17−23] however, much remains to be explored. A knowledge of the factors influencing base attack on metallaboranes is crucial to an understanding of the

(1) Shore, S. G. In *Boron Hydride Chemistry*; Muetterties, E. L., Ed.; Academic Press: New York, 1975; p 79.
(2) Kameda, M.; Shimoi, M.; Kodama, G. *Inorg. Chem.* **1984**, *23*, 3705−3709.
(3) Fratini, A. V.; Sullivan, G. W.; Denniston, M. L.; Hertz, R. K.; Shore, S. G. *J. Am. Chem. Soc.* **1974**, *96*, 3013.
(4) Paine, R. T.; Parry, R. W. *Inorg. Chem.* **1972**, *11*, 1237.
(5) Guter, G. A.; Schaeffer, G. W. *J. Am. Chem. Soc.* **1956**, *78*, 3546.
(6) *The Chemistry of Metal Cluster Complexes*; Shriver, D. F., Kaesz, H. D., Adams, R. D., Eds.; VCH: New York, 1990.
(7) Planalp, R. P.; Vahrenkamp, H. *Organometallics* **1987**, *6*, 492.
(8) Horwitz, C. P.; Holt, E. M.; Shriver, D. F. *Organometallics* **1985**, *4*, 1117.
(9) Beno, M. A.; Williams, J. M.; Tachikawa, M.; Muetterties, E. L. *J. Am. Chem. Soc.* **1981**, *103*, 1485.
(10) Ching, S.; Shriver, D. F. *J. Am. Chem. Soc.* **1989**, *111*, 3238.
(11) Housecroft, C. E.; Fehlner, T. P. *Adv. Organomet. Chem.* **1982**, *21*, 57.
(12) Kennedy, J. D. *Prog. Inorg. Chem.* **1984**, *32*, 519.
(13) Kennedy, J. D. *Prog. Inorg. Chem.* **1986**, *34*, 211.
(14) Grimes, R. N. In *Metal Interactions with Boron Clusters*; Grimes, R. N., Ed.; Plenum: New York, 1982; p 269.
(15) Deeming, A. J.; Kabir, S. E.; Powell, N. I.; Bates, P. A.; Hursthouse, M. B. *J. Chem. Soc., Dalton Trans.* **1987**, 1529.
(16) Crook, J. E.; Greenwood, N. N.; Kennedy, J. D.; McDonald, W. S. *Chem. Commun.* **1982**, 383.
(17) Housecroft, C. E.; Fehlner, T. P. *Inorg. Chem.* **1986**, *25*, 404.
(18) Housecroft, C. E.; Buhl, M. L.; Long, G. J.; Fehlner, T. P. *J. Am. Chem. Soc.* **1987**, *109*, 3323.
(19) Jan, D.-Y.; Workman, D. P.; Hsu, L.-Y.; Krause, J. A.; Shore, S. G. *Inorg. Chem.* **1992**, *31*, 5123.
(20) Barton, L.; Bould, J.; Fang, H.; Hupp, K.; Rath, N. P.; Gloeckner, C. *J. Am. Chem. Soc.* **1997**, *119*, 631.
(21) Macías, R.; Rath, N. P.; Barton, L. *Angew. Chem., Int. Ed.* **1999**, *38*, 162.
(22) McQuade, P.; Hupp, K.; Bould, J.; Fang, H.; Rath, N. P.; Thomas, R. L.; Barton, L. *Inorg. Chem.* **1999**, *38*, 5415.
(23) Kawano, Y.; Matsumoto, H.; Shimoi, M. *Chem. Lett.* **1999**, 489.

10.1021/om000667u CCC: $19.00
Publication on Web 11/08/2000

Chart 1

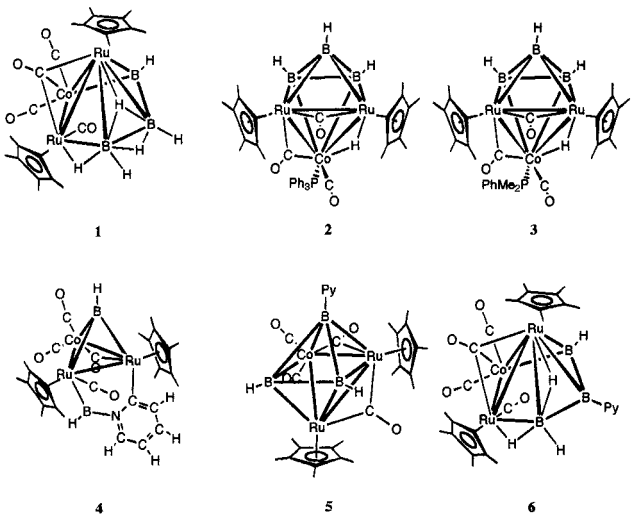

reactions of more complex Lewis bases such as unsaturated organic moieties.[24] Clearly one important factor will be the characteristics of the Lewis base, but other factors may play a role as well.

The discovery of a readily accessible route to metallaboranes containing monocyclopentadienyl metal fragments[25] permits the systematic study of their reaction chemistry. Herein we present the reaction chemistry of $\{Cp^*Ru\}\{Cp^*Ru(CO)\}\{Co(CO)_2\}(\mu\text{-}CO)B_3H_6$, **1**, $Cp^* = \eta^5\text{-}C_5Me_5$,[26] toward typical phosphorus and nitrogen bases. Compound **1** (Chart 1) is the major product derived from the reaction of $Co_2(CO)_8$ with $(Cp^*RuH)_2B_3H_7$. The reactivity of the parent $(Cp^*RuH)_2B_3H_7$ with Lewis bases is being explored by others, borane displacement being a prominent reaction pathway with phosphines.[23] With a metal carbonyl site, **1** offers the additional possibility of carbonyl substitution with a phosphine base. The reactions of pyridine with boranes[27] as well as metal clusters[28] generate interesting chemistry; however, in the competitive situation presented by a metallaborane, predictions are difficult. In the event, the stoichiometric chemistry carried out is complex. It is related to, but distinct from, that of boranes and metal clusters.

Results and Discussion

Reaction with Phosphines: Formation of $\{Cp^*Ru\}_2\{Co(CO)PPh_3\}(\mu\text{-}CO)_2B_3H_4$, 2, and $\{Cp^*Ru\}_2\{Co(CO)PMePh_2\}(\mu\text{-}CO)_2B_3H_4$, 3. The presence of carbonyl ligands in **1** suggests phosphine substitution as a likely reaction pathway. Metal and borane fragment displacement is also possible and has been observed previously in the reaction of both a ferraborane[17] and ruthenaborane[23] with phosphine Although **1** does not react with PPh_3 or PMe_2Ph in THF at room temperature (^{11}B and ^{31}P NMR), upon heating to 60 °C, a slow growth of two new resonances in a ratio of 1:2 was observed in the ^{11}B NMR spectrum. Only a single product **2** (or **3**) was produced, and the reaction was complete in 20 h. The molecular mass shows the replacement of one CO by PPh_3 (or PMe_2Ph) accompanied by the loss of H_2. On the basis of the spectroscopic data, the compound is formulated as a phosphine-substituted $\{Cp^*Ru\}_2\{Co(CO)_2\}(\mu\text{-}CO)(\mu^3\text{-}CO)B_3H_4$, a compound that was generated previously by simply heating **1**.[26] Thus, the overall reaction is

$$\mathbf{1} + PR_3 \rightarrow \{Cp^*Ru\}_2\{Co(CO)PPh_3\}(\mu\text{-}CO)_2B_3H_4\ (\mathbf{2}, \mathbf{3}) + CO + H_2$$

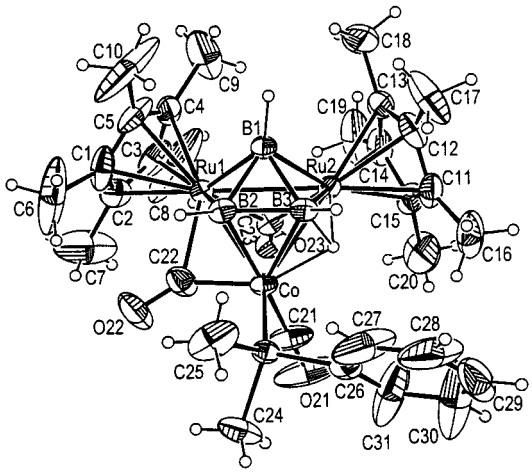

Figure 1. Structure of $\{Cp^*Ru\}_2\{Co(CO)PMePh_2\}(\mu\text{-}CO)_2B_3H_4$, **3**. Selected bond distances (Å): Ru1−Co 2.6348(8), Ru1−Ru2 2.7724(6), Ru1−C23 2.057(5), Ru1−C22 2.120(6), Ru1−B1 2.160(6), Ru1−B2 2.205(6), Ru2−C23 1.995(5), Ru2−B1 2.129(6), Ru2−Co 2.7028(8), Co−C21 1.766(7), Co−C22 1.794(7), Co−B2 2.112(6), Co−B3 2.149(6), Co−P 2.1564(14), B1−B2 1.747(9), B1−B3 1.751(8), B2−B3 1.709(9).

Although neither $\{Cp^*Ru\}_2\{Co(CO)_2\}(\mu\text{-}CO)(\mu^3\text{-}CO)B_3H_4$ nor **2** produced crystals suitable for a solid state structure, **3** did. The structure of **3** (Figure 1) shows an octahedral core consistent with seven skeletal electron pairs (sep).[29,30] The phosphine has replaced a terminal CO of the $Co(CO)_n$ fragment. The Ru_2Co triangle is preserved but is asymmetrically bridged. One carbonyl ligand bridges a Ru−Ru edge, and one a Ru−Co edge, making the two Cp*Ru fragments nonequivalent. The remaining edge is bridged by the endohydrogen atom, which, on the basis of the refinement, we suggest is triply bridging over a RuCoB face. As a consequence, the molecule is chiral. The bond distances and angles lie within normal ranges for this type of cluster.

The room-temperature NMR data require the existence of fluxionality in **2** and **3** that generates a virtual plane of symmetry: one Cp* signal, 1:2 ratio of boron signals, and, in **3**, a simple doublet for the methyl groups of the PMe_2Ph ligand. To further complicate matters, variable-temperature ^1H NMR on **3** showed the presence of two isomeric forms below −55 °C in a ratio of about

(24) Davan, T.; Corcoran, E. W., Jr.; Sneddon, L. G. *Organometallics* **1983**, *2*, 1693.
(25) Fehlner, T. P. *Organometallics* **2000**, *19*, 2643.
(26) Lei, X.; Shang, M.; Fehlner, T. P. *J. Am. Chem. Soc.* **1999**, *121*, 1275.
(27) Hawthorne, M. F.; Pitochelli, A. R. *J. Am. Chem. Soc.* **1961**, *80*, 6685.
(28) Johnson, B. F.; Lewis, J.; Nelson, W. J. H.; Pearsall, M. A.; Raithby, P. R.; Rosales, M. J.; McPartlin, M.; Sironi, A. *J. Chem. Soc., Dalton Trans.* **1987**, 327.
(29) Wade, K. *Adv. Inorg. Chem. Radiochem.* **1976**, *18*, 1.
(30) Mingos, D. M. P.; Wales, D. J. *Introduction to Cluster Chemistry*; Prentice Hall: New York, 1990.

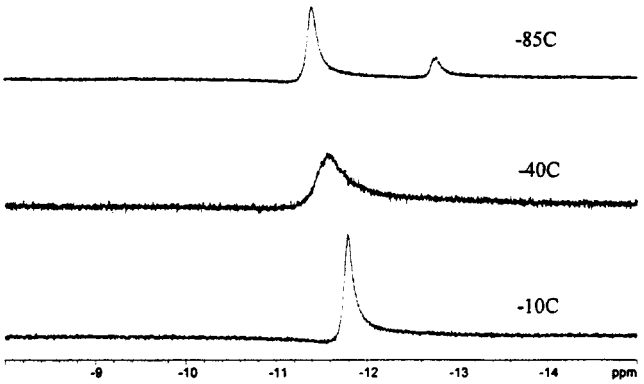

Figure 2. Variable-temperature ^{1}H NMR of $\{Cp^*Ru\}_2\{Co(CO)_2PMePh_2\}(\mu\text{-}CO)B_3H_4$, **3**, in toluene-$d_8$.

Chart 2

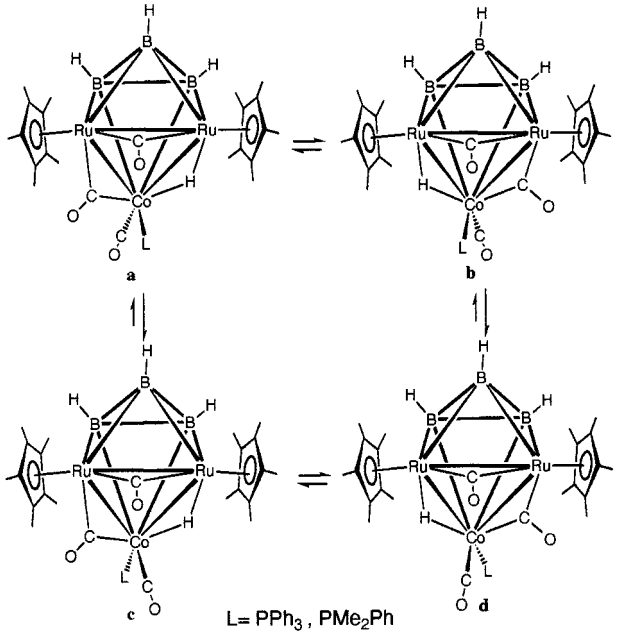

1:4. This is shown most clearly by the hydride resonance (Figure 2) but is supported by the presence of another Cp* signal to somewhat higher field plus another methyl resonance for the PMe_3Ph ligand to somewhat lower field, both with relative intensities corresponding to those observed for the hydride resonances. When the temperature is taken down to −100 °C, the major Cp* resonance splits into two signals of equal intensity (δ 1.78, 1.70) overlapped with the presumed two signals of the minor isomer, only one of which is observed (δ 1.66). The thermally decoupled BH(term) resonances exhibit a total of six maxima, also consistent with the presence of two nonfluxional forms of **3**.

The existence of the four species shown in Chart 2 provides an explanation for this behavior. The difference between **a**,**b** and **c**,**d**, the two isomer pairs, is the orientation of the phosphine and terminal CO on Co relative to the M_3 and B_3 triangles of the octahedron. The orientation illustrated by **c**,**d** is that found in the solid state structure of **3**, and presumably, this orientation corresponds to the most abundant isomer in solution. The difference between **a**,**c** and **b**,**d** is the positioning of the bridging H (shown as doubly bridging for simplicity) and a bridging CO relative to a plane that contains Co and B(1) and passes through the midpoint of the Ru−Ru bond; that is, they are mirror images. At the lowest temperature all four species are observed for **3**. As the temperature is raised, interconversion of the chiral pairs becomes rapid on the NMR time scale (**a** with **b**, **c** with **d**), and then, at higher temperature the interconversion of **a** and **c** as well as **b** and **c** becomes rapid.

In contrast, **2** shows only one kind of Cp* and one kind of hydride down to −90 °C. As the space available to the phosphine is larger when it is on the borane fragment side as found in the crystal structure, the bulkier PPh_3 derivative can only adopt the **c**,**d** form (no second isomer) and the rapid interconversion of **c** and **d** rationalizes the observed NMR behavior. This interpretation is confirmed by the infrared spectra. In addition to the bands displayed by **2**, **3** exhibits two more bands 30−50 cm^{-1} to lower energy of the terminal and bridging CO positions with intensities qualitatively comparable with those expected on the basis of the NMR experiments (Figure 2).

Under the conditions used in this work, slow substitution of a single CO ligand on the Co center takes place. The overall reaction also involves loss of H_2 as well as CO substitution; however, H_2 elimination probably precedes CO substitution. Heating **1** for 30 min yields $\{Cp^*Ru\}\{Cp^*Ru(CO)\}\{Co(CO)_2\}(\mu\text{-}CO)B_3H_4$, whereas the reaction with phosphine takes a day to reach completion. In contrast to the reaction of $(Cp^*RuH)_2B_3H_7$ with PMe_3,[23] there is no evidence for the formation of BH_3PR_3 despite the fact that the overall substitution reaction is rather sluggish. The steric bulk of the phosphine as well as its basicity may play a role here. The absence of competitive pathways contrasts with our earlier observations on the reaction of ferraboranes with the same phosphines.[17,18]

Reaction with Pyridine: Isolation of $\{(Cp^*Ru(CO)\}\{Co(CO)_2\}(\mu\text{-}CO)\{Cp^*Ru\}B_2H_2(NC_4H_4C)$, 4. As a nitrogen base might be expected to attack a boron site in preference to a metal site, we examined the reaction of **1** with pyridine under the conditions used for the reaction of **1** with phosphine. The reaction was both more facile and more complex. Attack at a boron site was evidenced by the formation of BH_3·py, and cluster degradation was confirmed by the presence of $\{Cp^*Ru(CO)H\}_2$ and $\{Cp^*Ru(CO)_2\}_2$ in the reaction mixture. In addition, the ^{11}B NMR of the reaction mixture indicated the presence of three new boron-containing compounds that formed as **1** disappeared. Column chromatography permitted the separation of the reaction mixture into two parts.

The first fraction contained a boron compound formed in low yield plus $\{Cp^*Ru(CO)H\}_2$. Upon slow evaporation of a hexane solution, red crystals of the boron compound were obtained along with dark red crystals of $\{Cp^*Ru(CO)H\}_2$, which were removed by washing with 2-propanol. ^{11}B and ^{1}H NMR spectra show that the new compound possesses two boron environments (ratio of 1:1), two kinds of Cp* (ratio of 1:1), and one py ligand (with only four protons the coordination mode of the py ligand was unclear). The ^{13}C NMR spectrum is consistent with the proton NMR and provides more information on the coordination mode of the py ligand. There are five carbon environments, four of which have terminal hydrogens, and therefore, one must be bonded

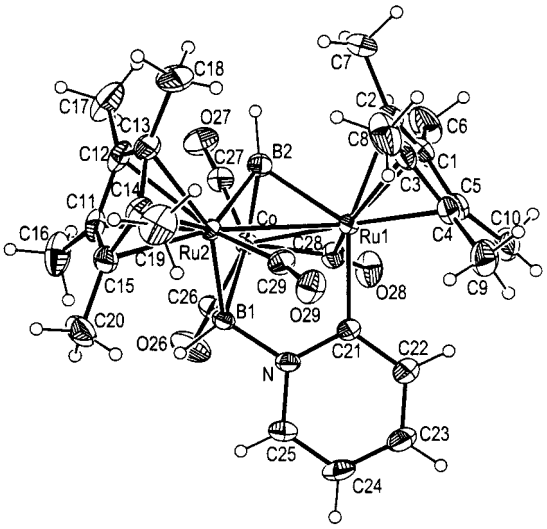

Figure 3. Structure of {(Cp*Ru(CO)}{Co(CO)$_2$}(μ-CO)-{Cp*Ru}B$_2$H$_2$(NC$_4$H$_4$C), **4**. Selected bond distances (Å): Ru1−Co 2.6242(7), Ru1−Ru2 2.8494(5), Ru1−C21 2.104(5), Ru1−B2 2.157(6), Ru1−C28 2.162(5), Ru1−C29 2.496(5), Ru2−C29 1.860(5), Ru2−B2 2.045(6), Ru2−B1 2.084(5), Ru2−Co 2.6265(7), Co−C28 1.834(5), Co−B2 2.036(6), Co−B1 2.194(5), B1−N 1.534(7).

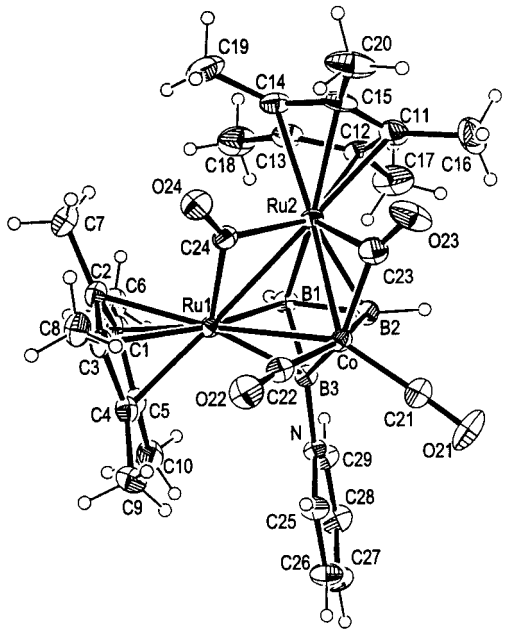

Figure 4. Structure of {Cp*Ru}$_2$}{Co(CO)$_2$}(μ-CO)$_2$B$_2$H$_2$B-(NC$_5$H$_5$), **5**. Selected bond distances (Å): Ru1−B3 2.140(4), Ru1−B1 2.166(4), Ru1−Co 2.6284(8), Ru1−Ru2 2.7276(10), Ru2−C24 2.045(4), Ru2−B1 2.181(4), Ru2−B2 2.192(4), Ru2−C23 2.201(4), Ru2−Co 2.6337(7), Co−C21 1.720(4), Co−C22 1.773(5), Co−C23 1.817(4), Co−B3 2.057(4), Co−B2 2.104(4), B1−B3 1.695(6), B1−B2 1.712(6), B2−B3 1.669(6), B3−N 1.539(5).

to either a boron or metal center. Combined with the mass spectrometric data the compound is formulated as {(Cp*Ru}$_2${Co(CO)$_4$}B$_2$H$_2$(NC$_4$H$_4$C), **4**, and the reaction is

$$\mathbf{1} + 2\text{py} \rightarrow \{\text{Cp*Ru}\}_2\text{Co(CO)}_4\text{B}_2\text{H}_2(\text{NC}_5\text{H}_4)\ (\mathbf{4}) + \text{BH}_3\cdot\text{py} + \text{H}_2$$

It required a solid state structure determination to uniquely define the compound as {(Cp*Ru(CO)}{Co-(CO)$_2$}(μ-CO){Cp*Ru}B$_2$H$_2$(NC$_4$H$_4$C), **4** (Figure 3). Considerable rearrangement has accompanied the loss of borane. The BH-capped Ru$_2$Co metal triangle generated has a Ru−Co edge bridged by a BHpy fragment. This py ligand has undergone an orthometalation reaction with the other ruthenium center yielding a five-membered Ru$_2$BNC ring. Presumably, **4** results from the displacement of BH$_3$ by py from **1** followed by addition of a second py to a boron center of the intermediate. Orthometalation and hydrogen elimination at the adjacent ruthenium center generates **4**. Although it is possible that the C(1) atom of py connects with B(2) while the N atom of py coordinates to Ru(1), the current structure is more reasonable based on the structure refinement as well as the characterization of product **5** discussed below. For the purposes of electron counting the bridging BHpy fragment is equivalent to a bridging CH$_2$. Thus, the four-atom cluster (BM$_3$) has 6 sep, in agreement with the observed tetrahedral structure. The bond distances and angles lie within normal ranges for this type of cluster.

Orthoboronation of metal-coordinated PPh$_3$ groups is known in metallaborane chemistry, as is orthometalation of similar ligands in organometallic complexes.[13,16] We are unaware of another example of orthometalation of a boron-coordinated pyridine. However, coordination of py to a boron atom adjacent to ruthenium generates a geometry similar to that found for Ph bound to P coordinated to a metal. Hence, the reaction is certainly a reasonable one.

Isolation of {Cp*Ru}$_2${Co(CO)$_2$}(μ-CO)$_2$B$_2$H$_2$B-(NC$_5$H$_5$), 5. The second fraction contained two boron-containing compounds (the major one plus another minor one) along with {Cp*Ru(CO)$_2$}$_2$. Upon slow evaporation of a hexane solution, black crystals were obtained along with yellow crystals of {Cp*Ru(CO)$_2$}$_2$, which were removed by washing with cold toluene. The ^{11}B NMR showed that the black crystals were not the major product but rather the second minor one. This compound exhibits three boron environments (1:1:1), one of which is a singlet, suggesting the presence of a Bpy fragment. The ^{1}H NMR shows two types of Cp* groups (1:1) and one intact, coordinated py ligand. When combined with the mass spectrometric data, the observations suggest the molecular formula {Cp*Ru}$_2$Co-(CO)$_4$B$_3$H$_2$(NC$_5$H$_5$), **5**. Thus, a parallel reaction taking place in this system is

$$\mathbf{1} + \text{py} \rightarrow \{\text{Cp*Ru}\}_2\text{Co(CO)}_4\text{B}_3\text{H}_2(\text{NC}_5\text{H}_5)\ (\mathbf{5}) + 2\text{H}_2$$

Effectively, the addition of py results in the elimination of H$_2$ and the replacement of H on B with py.

As a Bpy fragment is equivalent to a CH, this compound provides a straightforward application of the electron-counting rules: 7 sep suggest either an octahedral or capped square pyramidal cluster. The solid state structure (Figure 4) shows that the structure adoped is a closo-octahedron with a Ru$_2$Co metal triangle and a B$_3$ triangle reminiscent of those found in **3**. As one of the boron atoms lacks a terminal hydrogen and is coordinated with a py ligand, the

Chart 3

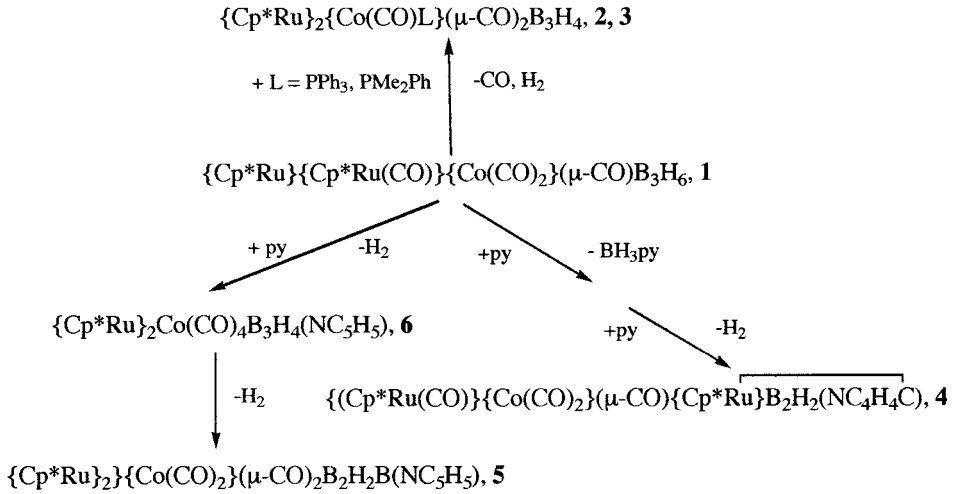

endohydrogen found in **3** is missing. The bond distances and angles lie within normal ranges for this type of cluster.

Unfortunately, all attempts to isolate the major boron-containing product, **6**, by fractional crystallization failed, as it decomposed within a couple of days at 0 °C. However, a partial spectroscopic characterization in a mixture, along with the two products already described, suggest a likely identity. Compound **6** shows three boron environments at δ 41.7(d), 52.7(s), and 74.6(d) in a 1:1:1 ratio. The proton NMR reveals two Cp* groups (δ 1.96, 1.55) and two types of M−H−B bridging hydrogens (δ −12.4 and −12.9). On this basis, the proposed formula for the compound is $\{Cp^*Ru\}_2Co(CO)_4B_3H_4(NC_5H_5)$, **6**, which could be formed by the reaction

$$\mathbf{1} + \text{py} \rightarrow \{Cp^*Ru\}_2Co(CO)_4B_3H_4(NC_5H_5)\ (\mathbf{6}) + H_2$$

Thus, it appears to be an intermediate on the way to **5**; however, being unable to obtain a pure sample, we were not able to establish this relationship unambiguously. With 8 sep the proposed structure is shown in Chart 1, where it is seen to be analogous to that of **1**: a Bpy fragment has replaced a HB−H− fragment.

With py as the base, the metal fragment of **1** is untouched. In one pathway, the py adds to the borane fragment and H_2 is eliminated, yielding **6** as the first product. Subsequent elimination of H_2, promoted by the presence of the coordinated py, generates **5**. As **4** contains a BHpy rather than a Bpy fragment, it is doubtful that it arises from **6**. Thus, in a parallel reaction, attack of py on **1** with elimination of BH_3py generates an unobserved intermediate. Subsequent attack of a second py with elimination of H_2 generates **4**. Thus, as summarized in Chart 3, reaction of **1** with phosphine results in attack at cobalt followed by CO displacement, whereas reaction with py results in attack at boron followed by competition between H_2 and BH_3 displacement.

Experimental Section

General Comments. All operations were conducted under argon atmosphere using standard Schlenk techniques. Solvents were distilled before use under N_2 as follows: sodium benzophenone ketyl for hexane, diethyl ether, and tetrahydrofuran. $[Cp^*RuCl_2]_2$ and $Co_2(CO)_8$ (Strem) was used as received. Silica gel (60−200 mesh) was purchased from J.T. Baker Inc. and dried at 140 °C before use. Chromatography was carried out on 3 cm of silica gel in a 2.5 cm diameter column. Spectra were recorded on the following: NMR, 300 or 500 MHz Varian FT-NMR spectrometer (reference, benzene, δ_H 7.15, solvent $[(Me_4N)(B_3H_8)]$ in acetone-d_6, δ_B, ppm, −29.7, external, H_3PO_4, δ_P, ppm, 0.0, external); IR, Nicolet 205 FT-IR spectrometer; MS, Finnigan MAT Model 8400 mass spectrometer (reference, perfluorokersene). Elemental analysis was performed by M-H-W Laboratories, Phoenix, AZ.

Synthesis. $\{Cp^*Ru\}_2\{Co(CO)PPh_3\}(\mu\text{-}CO)_2B_3H_4$, **2**. **1** (0.10 g, 0.14 mmol) and PPh_3 (0.04 g, 0.14 mmol) were loaded in a 100 mL Schlenk tube. Freshly distilled THF (5 mL) was slowly added to the mixture by plastic syringe. The reaction mixture was stirred for 20 h at 60 °C. Removal of the THF gave orange crystals, which were washed with hexane and dried to afford 0.08 g of red-orange microcrystals. The yield is 63% based on Ru.

Spectroscopic data: MS (EI): $P^+ = 916$, 3 B, 2 Ru atoms, fragment peaks corresponding to sequential loss of three CO. Calcd for weighted average of isotopomers lying within the instrument resolution, 916.1117, obsd, 916.1158. ^{11}B NMR (hexane, 22 °C): δ 88.0 (d, $J_{B-H} = 154$ Hz, $\{^1H\}$, s, 1B), 47.2 (d, $J_{B-H} = 60$, 130 Hz, $\{^1H\}$, s, 2B). ^{1}H NMR (C_6D_6, 22 °C): δ 8.50 (pcq, 1H, BH_t), 6.00 (pcq, 2H, BH_t), 7.73−7.00 (15H, P*Ph*$_3$), 1.67 (s, 30H, C_5Me_5), −11.39 (br, 1H, Ru-*H*-Ru). $^{31}P\{^1H\}$ NMR (C_6D_6, 22 °C): δ 56.3. IR (toluene, cm^{-1}): 2500 w, 2458 w (B−H); 1986 vs, 1793 s, 1736 s (CO). Anal. Calcd for $C_{41}H_{49}O_3B_3PCoRu_2$: C, 53.86, H, 5.40. Found: C, 53.80; H, 5.53.

$\{Cp^*Ru\}_2\{Co(CO)PMePh_2\}(\mu\text{-}CO)_2B_3H_4$, **3. 1** (0.10 g, 0.14 mmol) was loaded in a 100 mL Schlenk tube with 5 mL of freshly distilled THF. PMe_2Ph (0.04 g, 0.4 mL) was added by syringe and the reaction mixture stirred for 20 h at 60 °C. Column chromatography at room temperature with ether afforded a red solution, which was dried to give 0.05 g of red microcrystals. The yield is 42% based on Ru.

Spectroscopic data: MS (EI): $P^+ = 792$, 3 B, 2 Ru atoms, fragment peaks corresponding to sequential loss of three CO. Calcd for weighted average of isotopomers lying within the instrument resolution, 792.0804, obsd, 792.0776. ^{11}B NMR (hexane, 22 °C): δ 86.4 (d, $J_{B-H} = 141$ Hz, $\{^1H\}$, s, 1B), 44.3 (d, $J_{B-H} = 130$ Hz, $\{^1H\}$, s, 2B). ^{1}H NMR (C_6D_6, 22 °C): δ 8.63 (pcq, 1H, BH_t), 6.03 (pcq, 2H, BH_t), 7.40−7.02 (5H, PMe_2*Ph*), 1.70 (s, 30H, C_5Me_5), 1.50 (d, $H_{P-H} = 9$ Hz, 6H, P*Me*$_2$Ph), −11.73 (br, 1H, Ru−*H*−Ru). $^{31}P\{^1H\}$ NMR (C_6D_6, 22 °C): δ 24.3. IR (hexane, cm^{-1}): 2482 w, 2453 w (B−H); 1991 vs, 1797 s, 1738 s (CO): minor isomer 1937 s, 1764 w (CO). Anal. Calcd for $C_{31}H_{45}O_3B_3PCoRu_2$: C, 47.12; H, 5.74. Found: C, 47.22; H, 5.77.

Table 1. Crystal Data and Structure Refinement for {Cp*Ru}$_2${Co(CO)PMePh$_2$}(μ-CO)$_2$B$_3$H$_4$, 3, {(Cp*Ru(CO)}{Co(CO)$_2$}(μ-CO){Cp*Ru}B$_2$H$_2$(NC$_4$H$_4$C), 4, and {Cp*Ru}$_2${Co(CO)$_2$}(μ-CO)$_2$B$_2$H$_2$B(NC$_5$H$_5$), 5

empirical formula	C31 H45 B3 Co O3 P Ru2	C29 H36 B2 Co N O4 Ru2	C29 H37 B3 Co N O4 Ru2
fw	790.14	745.28	757.10
temp	293(2) K	293(2) K	293(2) K
wavelength	0.71073 Å	0.71073 Å	0.71073 Å
cryst syst	monoclinic	orthorhombic	triclinic
space group	P2(1)/c	*Pbca*	P-1
unit cell dimens	a = 10.3801(6) Å	a = 17.0349(15) Å	a = 8.7880(14) Å, α = 97.418(19)°
	b = 16.7455(14) Å	b = 15.7770(13) Å	b = 9.276(2) Å, β = 97.89(2)°
	c = 19.455(2) Å, β = 95.940(6)°	c = 22.1476(16) Å	c = 20.171(3) Å γ = 111.350(15)°
volume	3363.6(4) Å^3	5952.4(8) Å^3	1488.1(5) Å^3
Z	4	8	2
density (calcd)	1.563 Mg/m^3	1.663 Mg/m^3	1.690 Mg/m^3
abs coeff	1.454 mm^{-1}	1.587 mm^{-1}	1.588 mm^{-1}
F(000)	1600	2992	760
cryst size	0.25 × 0.20 × 0.18 mm	0.32 × 0.15 × 0.11 mm^3	0.51 × 0.10 × 0.07 mm^3
θ range for data collection	2.10−24.98°	2.19−24.99°	2.08−25.32°
index ranges	$-12\le h\le 12$, $0\le k\le 19$, $0\le l\le 23$	$0\le h\le 20$, $0\le k\le 18$, $0\le l\le 26$	$0\le h\le 10$, $-11\le k\le 10$, $-23\le l\le 23$
no. of reflns collected	6076	5232	5276
no. of ind reflns	5899 [R(int) = 0.0138]	5232 [R(int) = 0.0000]	5276 [R(int) = 0.0000]
no. of abs corr	semiempirical from ψ-scans	empirical	empirical
max. and min. transmn	0.9990 and 0.9031	0.9995 and 0.8821	0.7988 and 0.7592
refinement method	full-matrix on F^2	full-matrix least-squares on F^2	full-matrix least-squares on F^2
no. of data/restraints/params	5898/5/370	5232/2/358	5276/2/367
goodness-of-fit on F^2	1.003	1.047	1.050
final R indices [$I>2\sigma(I)$]	R1 = 0.0415, wR2 = 0.1095	R1 = 0.0368, wR2 = 0.0847	R1 = 0.0399, wR2 = 0.1021
R indices (all data)	R1 = 0.0527, wR2 = 0.1200	R1 = 0.0563, wR2 = 0.0936	R1 = 0.0466, wR2 = 0.1078
largest diff peak and hole	2.007 and −0.596 e Å^{-3}	0.778 and −0.441 e Å^{-3}	1.169 and −1.515 e Å^{-3}

{(Cp*Ru(CO)}{Co(CO)$_2$}(μ-CO){Cp*Ru}B$_2$H$_2$(NC$_4$H$_4$C), 4, and {Cp*Ru}$_2${Co(CO)$_2$}(μ-CO)$_2$B$_2$H$_2$B(NC$_5$H$_5$), 5. **1** (0.10 g, 0.14 mmol) was loaded in a 100 mL Schlenk tube with 5 mL of freshly distilled THF. Pyridine (0.28 mmol, 22 μL) was then added by syringe and the reaction mixture stirred for 2 h at 60 °C. NMR data showed the presence of at least three new boron compounds as well as {(C$_5$Me$_5$)Ru(CO)$_2$}$_2$ and {(C$_5$Me$_5$)RuH(CO)}$_2$. Column chromatography was performed at room temperature. Elution with 5% ether in hexane afforded a red solution, which was dried to give a dark red solid, which contained one new boron-containing compound. Fractional crystallization yielded red crystals. The dark red crystals of **4** were washed with 2-propanol, collected, and dried (∼5 mg, 5% based on Ru). Subsequent elution with ether gave a dark brown solution which contained two boron compounds. Slow evaporation gave black crystals with a brown solid. The black crystals of **5** were washed with toluene, collected, and dried (∼10 mg, 10% based on Ru).

Spectroscopic data for **4**: MS (EI), P$^+$ = 747, 2 B, 2 Ru atoms, fragment peaks corresponding to sequential loss of four CO. Calcd for weighted average of isotopomers lying within the instrument resolution, 747.0249, obsd, 747.0270. ^{11}B NMR (hexane, 22 °C): δ 113.2 (b, {^{1}H}, s, 1B), 64.2 (b, {^{1}H}, s, 2B). ^{1}H NMR (acetone-d_6, 22 °C): δ 8.53, 8.09, 7.40, 6.91 (4H, NC$_5$H$_4$), 7.48 (pcq, 1H, BH$_t$), 6.89 (pcq, 1H, BH$_t$), 1.91 (s, 15H, C$_5$*Me*$_5$), 1.70 (s, 15H, C$_5$*Me*$_5$). ^{13}C NMR (acetone-d_6, 22 °C): δ 226.3 (CO), 153.4, 143.4, 139.1,133.9, 117.3 (N*C*$_5$H$_4$), 100.1, 98.1(*C*$_5$Me$_5$), 11.1, 9.7 (C$_5$*Me*$_5$). IR (hexane, cm^{-1}): 2528 w, 2416 w (B−H); 1987 s, 1947 s, 1936 s, 1833 m, 1764 m (CO).

Spectroscopic data for **5**: MS (EI), P$^+$ = 760, 3 B, 2 Ru atoms. Calcd for weighted average of isotopomers lying within the instrument resolution, 760.0499, obsd, 760.0493. ^{11}B NMR (hexane, 22 °C): δ 77.5 (b, {^{1}H}, s, 1B), 76.4 (s, 1B), 66.5 (b, {^{1}H}, s, 1B). ^{1}H NMR (C$_6$D$_6$, 22 °C): δ 8.41, 6.46, 6.12 (5H, NC$_5$H$_5$), 8.52 (pcq, 1H, BH$_t$), 7.73 (pcq, 1H, BH$_t$), 1.79 (s, 15H, C$_5$*Me*$_5$), 1.42 (s, 15H, C$_5$*Me*$_5$). IR (hexane, cm^{-1}): 2449 w, 2406 w (B−H); 1973 vs, 1922 s, 1847 m, 1737 s (CO). Anal. Calcd for C$_{29}$H$_{37}$O$_4$B$_3$NCoRu$_2$: C, 46.01; H, 4.93; N, 1.85. Found: C, 46.26; H, 5.15; N, 1.69

Structure Determinations. {Cp*Ru}$_2${Co(CO)PMePh$_2$}(μ-CO)$_2$B$_3$H$_4$, 3. Dark red block-like crystals suitable for X-ray diffraction were obtained by keeping a hexane solution at 10 °C for several days. The crystal data are given in Table 1. Structure solution and refinement were performed on a PC by using the SHELXTL package. Most of the nonhydrogen atoms were located by the direct method; the remaining nonhydrogen atoms were found in succeeding difference Fourier syntheses. Least-squares refinement was carried out on F^2 for all reflections. The phenyl group was refined to fit a regular hexagon with the C−C distance 1.39 Å. In the final refinement hydrogen atoms for the pentamethylcyclopentadienyl groups were refined with an idealized riding model that restrained the C−H distance to 0.96 Å and the isotropic thermal parameter of a hydrogen atom to 1.5 times the equivalent isotropic thermal parameter of its bonded carbon atom. All reflections, including those with negative intensities, were included in the refinement, and the $I > 2\sigma(I)$ criterion was used only for calculating R1.

{(Cp*Ru(CO)}{Co(CO)$_2$}(μ-CO){Cp*Ru}B$_2$H$_2$(NC$_4$H$_4$C), 4, Dark red crystals suitable for X-ray diffraction were obtained by slowly evaporating a saturated toluene solution at room temperature under N$_2$ for 3 days. The crystal data are given in Table 1. Most of the nonhydrogen atoms were located by the direct method; the remaining nonhydrogen atoms were found in succeeding difference Fourier syntheses. In the final refinement hydrogen atoms for the pentamethylcyclopentadienyl groups were refined with an idealized riding model, which restrained the C−H distance to 0.96 Å and the isotropic thermal parameter of a hydrogen atom to 1.5 times the equivalent isotropic thermal parameter of its bonded

carbon atom. After all non-hydrogen atoms were refined anisotropically and hydrogen atoms of pentamethylcyclopentadienyl groups refined isotropically, difference Fourier synthesis located the rest of the B−H terminal hydrogen atoms, which were refined isotropically with bond length restraints, which used four free variables in the refinement to confine B−H bond distances around their mean values. All reflections, including those with negative intensities, were included in the refinement, and the $I > 2\sigma(I)$ criterion was used only for calculating R1.

{Cp*Ru}$_2$}{Co(CO)$_2$}(μ-CO)$_2$B$_2$H$_2$B(NC$_5$H$_5$), 5. Black crystals suitable for X-ray diffraction were obtained by slowly evaporating a saturated toluene solution at room temperature under N_2 for 3 days. The crystal data are given in Table 1, and the structure solution and refinement were carried out in the same manner as with **4**.

Acknowledgment. We thank the National Science Foundation for generous support of this research.

Supporting Information Available: Tables of crystal data, atomic coordinates and isotropic displacement parameters, bond lengths and angles, and anisotropic displacement parameters for **3**, **4**, and **5**. This material is available free of charge via the Internet at http://pubs.acs.org.

OM000667U